Serotonin 2A receptor disulfide bridge integrity is crucial for ligand binding to different signalling states

Alba Iglesias[1], Marta Cimadevila[1], Rocío Ailim de la Fuente[1,2], María Martí-Solano[3], María Isabel Cadavid[1], Marián Castro[1,2], Jana Selent[3], María Isabel Loza[1]*, José Brea[1]*

[1]BioFarma Research Group, [2]Molecular Pharmacology of G protein-coupled receptors laboratory, Centro Singular de Investigación en Medicina Molecular y Enfermedades Crónicas (CIMUS), Universidade de Santiago de Compostela, Avenida de Barcelona 22, 15782, Santiago de Compostela, Spain.

[3]GPCR drug discovery group, Research Programme on Biomedical Informatics (GRIB), Hospital del Mar Medical Research Institute (IMIM) - Department of Experimental and Health Sciences of Pompeu Fabra University (UPF), Barcelona, Spain

Corresponding author name: María Isabel Loza García, e-mail: mabel.loza@usc.es;

José Manuel Brea Floriani, e-mail: pepo.brea@usc.es

Phone number: +34 881815459, +34 881815460

Contact information: mabel.loza@usc.es; pepo.brea@usc.es

Category: Neuropharmacology

Abstract

The serotonin 2_A (5-HT_{2A}) receptor, is a class A G-protein coupled receptor (GPCR) associated with central nervous system pathologies such as schizophrenia. A disulfide bond connecting the extracellular loop 2 (ECL-2) and the top of transmembrane (TM) helix 3 is found in >90% of all GPCRs and has been suggested to be important for receptor conformation and ligand recognition and function. The 5-HT_{2A} conserved disulfide bridge is formed by Cys^{148} (TM3) and Cys^{227} (ECL-2). We hypothesized that this disulfide bridge may determine 5-HT_{2A} receptor functions such as receptor activation, functional selectivity and ligand recognition. We used the reducing agent dithiothreitol (DTT) to enable us to determine how the reduction of disulfide bridges affects radioligand binding, second messenger mobilization and receptor dimerization. We observed a DTT-induced decrease in the number of binding sites (1190 ± 63.55 fmol/mg prot for control cells compared with 921.2 ± 60.84 fmol/mg prot for DTT-treated cells) as well as in the efficacy of both signalling pathways

characterized, although the affinity and potency were unchanged. In molecular dynamic simulations, the ECL-2 of the receptor with a broken cysteine bond adopts a wider variety of conformations, some of which protrude deeper into the receptor orthosteric binding pocket leading to collapse of the pocket. A shrunken binding pocket would be incapable of accommodating LSD. Our findings show that the disulfide bridge between TM3 and ECL-2 is essential for 5-HT_{2A} receptor signalling. This reveals the integrity of the ECL-2 epitope, which should be explored in the development of novel ligands acting as allosteric modulators of 5-HT_{2A} receptors.

Keywords: 5-HT_{2A} receptors, phospholipase A_2, phospholipase C, radioligand binding, disulfide bridges, dithiothreitol

Chemical compounds studied in this article

DL-1,4-Dithiothreitol (PubChem CID: 446094); Serotonin hydrochloride (PubChem CID: 160436); Clozapine (PubChem CID: 2818); Methysergide maleate (PubChem CID: 5281073); [3H]LSD (PubChem CID: 44559100)

1. Introduction

G-protein coupled receptors (GPCRs) represent the largest family of cell surface proteins encoded by the human genome and are involved in signalling across biological membranes. GPCRs bind different types of ligands, such as photons, ions, hormones, peptides, nucleotides and biogenic amines. They can thus modulate a wide range of physiological processes and are involved in numerous diseases. Mammalian GPCRs can be classified into three major classes (A, B and C) on the basis of sequence similarity. The largest of these, class A, includes the prototypical rhodopsin and the biogenic amine GPCRs. All GPCRs share a common structure, including an extracellular N-terminus, seven-α-helix transmembrane regions connected by three alternating extracellular loops (ECL1-3), three intracellular loops (ICL1-3) and an intracellular C-terminus. A disulfide bond connecting the ECL-2 and the top of transmembrane (TM) helix 3 is found in >90% of all GPCRs and has been suggested to be important for receptor conformation and ligand recognition and functioning [1-7]. Other disulfide bonds in the extracellular side have been described for different receptors [8].

The GPCRs are known to exist as collections of conformations in equilibrium, and their ligand potency and efficacy are associated with their absolute and relative affinity for the different conformations adopted by the receptor [9]. Agonists (full or partial) and positive allosteric modulators have been found to be able to select the different active conformations of GPCRs, thus leading to the agonist-dependent differential regulation of signalling pathways. This effect has been described as “agonist-directed trafficking of receptor stimulus” [10], “biased agonism” [11], “functional selectivity” [12] and “collateral efficacy” [13].

The serotonin 2_A receptor (5-HT_{2A}) is a class A GPCR associated with central nervous system pathologies such as schizophrenia and is an important target for atypical antipsychotic drugs [14, 15]. The 5-HT_{2A} receptor was one of the first types of GPCR for which the functional selectivity phenomenon was observed, with different ligands differentially activating

phospholipase A_2 (PLA_2) - inducing arachidonic acid (AA) release - and phospholipase C (PLC) - resulting in the production of inositol phosphate (IP) formation and diacylglycerol (DAG) - for the same receptor [12, 16-18].

We have previously demonstrated the existence of 5-HT_{2A} homo-oligomers in the human brain and in recombinant cell lines [19]. The oligomerization was demonstrated by a negative cooperativity phenomenon observed for certain ligands, such as clozapine, through the PLA_2 signalling pathway, while other ligands, such as haloperidol, demonstrated no cooperativity between protomers in this pathway. Negative cooperativity between the binding sites of two protomers has already been described for various class-A GPCRs. The binding of a ligand to an orthosteric centre thus hinders the binding of a second ligand to another orthosteric centre of the dimer [19-21]. Interestingly, in contrast to its effects on the PLA_2 signalling pathway, no cooperativity for clozapine was observed in the PLC-mediated pathway [19, 21].

From a structural viewpoint, the 5-HT_{2A} receptor constitutes a typical class A GPCR. It contains a total of fifteen cysteines, seven on the extracellular side and one at the top of TM3. The GPCR conserved disulfide bridge is formed by Cys^{148} (TM3) and Cys^{227} (ECL-2) (**Fig. 1**).

Recent reports indicate that LSD displays slow binding kinetics at 5-HT_{2A} and 5-HT_{2B} receptors. In view of the 5-HT_{2B} crystal structure, it has been proposed that this may be due to a lid formed by ECL-2 at the entrance to the binding pocket. A mutation (L229A) in ECL-2 increases the mobility of this lid and greatly accelerates LSD binding kinetics and selectively dampens β-arrestin2 recruitment [22].

We hypothesized that this disulfide bridge may determine 5-HT_{2A} receptor functions such as receptor activation, functional selectivity and ligand recognition. The aim of this study was to characterize the effect of the reduction in the number of disulfide bridges in the 5-HT_{2A}

receptor, in relation to their contribution to ligand binding, receptor activation and homodimer formation.

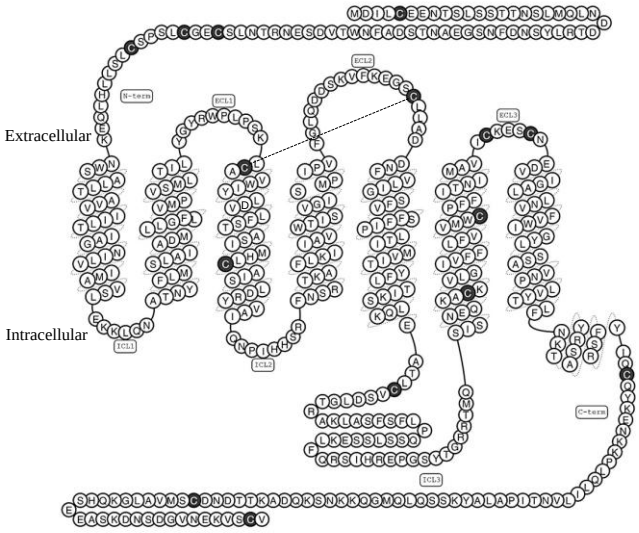

Fig. 1. A secondary structure model of the human 5-HT_{2A} receptor. The location of 15 cysteine residues (black circles) and the conserved disulfide bridge are indicated (modified from www.gpcrdb.org).

2. Material and Methods

2.1. Drugs and reagents

[^{3}H]LSD (83.6 Ci/mmol), [^{3}H]*myo*-Inositol (20.3 Ci/mmol) and [^{14}C]arachidonic acid (57.1 mCi/mmol) were purchased from PerkinElmer Life Science (Waltham, Massachusetts). DL-1,4-Dithiothreitol (DTT)**,** clozapine, methysergide maleate and serotonin hydrochloride (5-HT) were purchased from Sigma Aldrich (St. Louis, Missouri). RNA Binding YSi SPA Beads and OptiPhase Supermix scintillation cocktail were purchased from Perkin Elmer (Waltham, Massachusetts). Bovine Serum Albumin (BSA) Fraction V fatty acid free was purchased from Roche (Basel, Switzerland). MultiScreen® Filter Plates were purchased from Millipore (Billerica, Massachusetts). All other reagents were purchased from Sigma Aldrich.

2.2. Cell culture

Cells were grown at 37 ºC in a 5% CO_2 humidified atmosphere. Chinese hamster ovary cells stably expressing human 5-HT_{2A} receptors at a density of~ 200 fmol/mg protein (CHO-FA4 cells) (passages between 12 and 25) were maintained in standard tissue culture plates (150 mm in diameter) in Dulbecco's Modified Eagle's Medium-F12 (DMEM-F12; Gibco) supplemented with 10% (v/v) foetal bovine serum (FBS; Sigma Aldrich), 1% L-glutamine (Sigma Aldrich), 100 U/ml penicillin/0.1mg/ml streptomycin (Sigma Aldrich) and 300 µg/ml hygromycin (Invitrogen).

Human Embryonic Kidney 293T cells (HEK 293T) (passages between 10 and 18) were maintained in standard tissue culture plates (150 mm in diameter) in Dulbecco's Modified Eagle's Medium (DMEM; Sigma Aldrich) supplemented with 10% (v/v) FBS, 1% (v/v) Glutamax (Gibco) and 100 U/ml penicillin/0.1 mg/ml streptomycin.

2.3. Membrane preparations of human 5-HT_{2A} receptors

Prior to being harvested, stably transfected cells were grown for 24 h in DMEM-F12 supplemented with 10% (v/v) dialyzed FBS without hygromycin. The culture medium was

aspirated and the cells were washed twice with ice-cold phosphate buffered saline (PBS) before being scraped from the culture plate in PBS and pelleted by centrifugation at 800 x *g*, 15 min at 4 ºC. The cell pellet was resuspended in PBS or PBS supplemented with 20 mM DTT and incubated for 10 min at 37 ºC. The cell suspension was then centrifuged under the same conditions. The cell pellet was washed in ice-cold PBS, resuspended in 50 mM Tris-HCl, pH= 7.5 at 4 ºC, and homogenized with a Polytron homogenizer. The homogenate was centrifuged at 48000 x *g* for 40 min at 4 ºC and the resulting pellet was resuspended in 50 mM Tris-HCl, pH= 7.5, at 4ºC. The protein concentration was determined by the Bradford method with the Bio-Rad Protein Assay (Bio-Rad, California) and bovine serum albumin as standard.

2.4. Saturation binding assays with human 5-HT$_{2A}$ receptors

Membranes obtained from CHO-FA4 expressing 5-HT$_{2A}$ receptors prepared either in the absence or presence of 20 mM DTT were incubated with eight different concentrations of [^{3}H]LSD (83.6 Ci/mmol) in the range 0.16-20 nM (80 µg of protein per well) in the incubation buffer (50 mM Tris-HCl, pH= 7.5). Non-specific binding was determined by the addition of 1 µM methysergide. The reaction mixture was incubated at 37 °C for 30 min. The reaction samples were transferred to a multiscreen GF/B 96-well plate (Millipore) pretreated with 0.5% polyethylenimine (PEI, Sigma Aldrich) and were then filtered and washed six times with 250 µl wash buffer (50 mM Tris-HCl, pH 6.6). The filters were dried and 30 µl Universol (MP Biomedicals, Santa Ana, California) was added to each well. The radioactivity was detected in a microplate beta scintillation counter (Microbeta Trilux, PerkinElmer).

2.5. Binding kinetics: determination of association and dissociation rates

Membranes obtained from CHO-FA4 expressing 5-HT$_{2A}$ receptors prepared either in the absence or presence of 20 mM DTT were incubated in 50 mM Tris-HCl (pH 7.5) and 1 nM [^{3}H]LSD (83.6 Ci/mmol) in a 96 well plate (80 µg of protein per well) at 37 ºC. Association was measured at different times between 0 and 60 minutes, and dissociation was initiated 30

minutes later by addition of 1 µM methysergide at different times between 0 and 180 minutes. Non-specific binding was measured in the presence of 1 µM methysergide. Samples were transferred to a multiscreen GF/B 96-well plate pretreated with 0.5% PEI and were then filtered and washed six times with 250 µl wash buffer (50 mM Tris-HCl, pH 6.6). The filters were dried and 30 µl Universol was added to each well. The radioactivity was detected in a microplate beta scintillation counter (Microbeta Trilux, PerkinElmer).

2.6. Competition binding to human 5-HT$_{2A}$ receptors

Serotonin 5-HT$_{2A}$ receptor competition binding experiments were carried out with membranes from CHO-5-HT$_{2A}$ cells that were either pretreated or not pretreated with 20 mM DTT (in the preparation protocol). On the day of the assay, membranes were defrosted and resuspended in incubation buffer (50 mM Tris-HCl, pH 7.5). Each reaction well of a 96-well plate contained 80 µg of protein, 1 nM [^{3}H]LSD (83.6 Ci/mmol) and different concentrations of clozapine. Non-specific binding was determined in the presence of 1 µM methysergide. The reaction mixture was incubated at 37 °C for 30 min. The samples were transferred to multiscreen GF/B 96-well plate (Millipore) pretreated with 0.5% PEI and were then filtered and washed six times with 250 µl wash buffer (50 mM Tris-HCl, pH 6.6). The filters were dried and 30 µl Universol was added to each well. The radioactivity was detected in a microplate beta scintillation counter (Microbeta Trilux, PerkinElmer).

2.7. Measurement of effect of treatment with 20 mM DTT on AA release and IP accumulation in CHO-FA4 cells expressing human 5-HT$_{2A}$ receptors

Measurement of AA release and IP accumulation was performed simultaneously in the same well, as previously described [21].

Cells were seeded into 96-well tissue culture plates at a density of 2x10^4 cells/well. After 24 h, the medium was replaced with serum-free medium containing 10 µCi/ml [^{3}H]*myo*-inositol

(20.3 Ci/mmol) for 24 h and 0.2 μCi/ml [^{14}C]arachidonic acid (57.1 mCi/mmol) for 4 h at 37 ºC.

After the labelling period, control cells were washed for 10 min at 37 ºC with Hanks' Balanced Salt Solution (HBSS, Sigma Aldrich) supplemented with 20 mM HEPES, 20 mM LiCl and 2% fatty acid free BSA (experimental medium). Treated cells were washed with experimental medium supplemented with 20 mM DTT. The cells were then incubated for 20 min with experimental medium at 37 ºC containing vehicle or the indicated concentrations of drugs (clozapine and 5-HT). At the end of the incubation time, 90 μl of medium was added to the flexiplate with 150 μl OptiPhase SuperMix cocktail for measurement of [^{14}C]AA release. The medium was discarded and 200 μl of 100 mM formic acid was added to the cells for 30 min at 4ºC, then 20 μl were added to the flexiplate with 80 μl of a solution of RNA Binding YSi SPA beads for measurement of the accumulation of [^{3}H]IPs from the cells (IP_1, IP_2, and IP_3, collectively referred to as IPs). The radioactivity was quantified with a liquid scintillation counter (WALLAC Microbeta TriLux 1450-023).

2.8. Bioluminiscence resonance energy transfer (BRET) assays for assessment of receptor dimerization

BRET methodology is based on the fact that the degree of physical proximity (< 100 Å) between molecules can be assessed in living cells by the level of energy transfer between the energy donor *Renilla* luciferase (RLuc) and a fluorescence acceptor, the yellow fluorescence protein (YFP). BRET saturation experiments were performed using HEK293T cells previously seeded into 100-mm dishes at a density of $2x10^6$ cells and transfected 24 h later with a fixed amount of RLuc-N2-5-HT_{2A} luciferase donor plasmid (0.06 μg DNA/dish) and with increasing amounts of pcDNA3-5-HT_{2A}-YFP acceptor plasmid (from 0.06 to 4 μg DNA/dish) by using linear polyethylenimine MW-25000 at a DNA/polyethylenimine ratio of 1:6 [23]. In each transfection mix, the total amount of DNA was maintained constant by the

addition of empty vector up to 5 μg. The transfection medium was aspirated 24 hours after transfection. The cells were then washed with PBS and $5x10^4$ cells/well were seeded in a 96-well plate pretreated with 0.1 mg/ml poly-D-lysine hydrobromide (Sigma Aldrich). Forty-eight hours post transfection, the cells were washed with HBSS and incubated with HBSS or HBSS supplemented with 20 mM DTT for 10 min at 37 ºC. The YFP expression was then quantified in each well by direct measurement of fluorescence emission at 530 nm (excitation wavelength of 480 nm). The buffer was removed and coelenterazine *h* (Molecular Probes) was added to a final concentration of 5 μM in HBSS. The plate was incubated for 10 min at 37 ºC in darkness and BRET was subsequently quantified by dual bioluminescence measurement (370-480 nm for RLuc emission and 520-570 nm for YFP emission). Ten minutes later, total luminescence (400-700 nm) was quantified as a measure of donor expression. All measurements were performed in an Infinite® M1000Pro (TECAN) microplate reader. The BRET ratio was calculated as emission at 520-570 nm/emission at 370-480 nm. Net BRET was defined as the 530 nm/485 nm ratio of cells co-expressing donor (RLuc) and acceptor (YFP) plasmid constructs minus the BRET ratio of cells expressing only the donor (RLuc) plasmid construct in the same experiment. Results were expressed as milli net BRET units (mBU), which correspond to the net BRET ratio values multiplied by 1000. BRET saturation curves were obtained by representing mBU as a function of the acceptor expression/donor expression, as determined by direct quantification of fluorescence and total luminescence emission. Data were fitted to the hyperbolic function (one binding site) with GraphPad Prism 4.0 software. The equation parameters B_{max} and K_d corresponded respectively to the maximal BRET signal obtained ($BRET_{max}$) and $BRET_{50}$, i.e. the acceptor/donor ratio providing 50% of the $BRET_{max}$.

2.9. In silico structural model of ECL-2 on 5-HT$_{2A}$ receptor before and after disruption of the Cys^{148}-bond

In order to build a 5-HT_{2A} receptor model, we used the recently determined structure of the related 5-HT_{2B} receptor in complex with LSD (PDB ID 5TVN) as template. We first aligned the Uniprot sequence of the 5-HT_{2A} receptor to the one of the 5-HT_{2B} receptors with MOE software (Molecular Operating Environment (MOE) software, http://www.chemcomp.com/software.htm). We then built a homology model and optimized the model with the AMBER12:EHT force field included in the MOE software [24]. Finally, the model was stereochemically validated with PROCHECK [25].

In order to evaluate the conformational space of the ECL-2 with an intact and broken cysteine bond, we explored both conditions by performing a Low Mode Search analysis of this region with MOE software (with the AMBER12:EHT force field, Born solvation and a temperature of 300 K). The following conditions were applied for the Low Mode Search: rejection limit of 100, iteration limit of 500, RMSD gradient of 0.1 and maximum number of energy minimization iterations of 500. The tolerance for equal conformations was set to a RMSD of 1, while the energy window was set to 100. Using these settings, we obtained 495 conformations for the receptor with a broken disulfide bridge and 490 different conformations for the receptor with an intact disulfide bridge. From this pool of conformations, we selected the best 200 conformations in terms of energy and depicted them by a stride of 2 in Figure 8.

2.10. Data analysis

Nonlinear fitting of the concentration-response curves was conducted with Prism 4.0 software (GraphPad Software, La Jolla, USA) by applying both a four-parameter logistic equation and a two-site competition equation. Dissociation and association kinetic data were fitted to a one-phase exponential decay equation and a one-phase exponential association equation, respectively. Statistical comparisons between fits were performed by extra sum-of-squares *F* test [26]. Statistical significance was set at $P < 0.05$. Statistical comparisons between binding and functional parameters (treated relative to control) were performed by Student's *t*-test with

SPSS statistics 20 (IBM). Statistical significance was set at $P < 0.05$. The following equation was used to calculate k_{on}:

$$k_{on} = \frac{k_{ob} - k_{off}}{[radioligand(nM)]}$$

3. Results

3.1. Treatment of 5-HT$_{2A}$ receptors with DTT modified ligand binding properties

To investigate the effect of DTT on ligand binding properties of the 5-HT$_{2A}$ receptor, radioligand binding assays (saturation, kinetic and competition assays) were conducted with [^{3}H]LSD in the presence and absence of 20 mM DTT. Representative saturation isotherms for 5-HT$_{2A}$ receptor, with either buffer or DTT treatment, are shown in **Figure 2**. DTT treatment induced a statistically significant decrease in the maximum number of binding sites (B_{max}) ($P < 0.05$, Student's *t* test) without affecting the equilibrium dissociation constant (K_d) (**Fig 2**; **Table 1**).

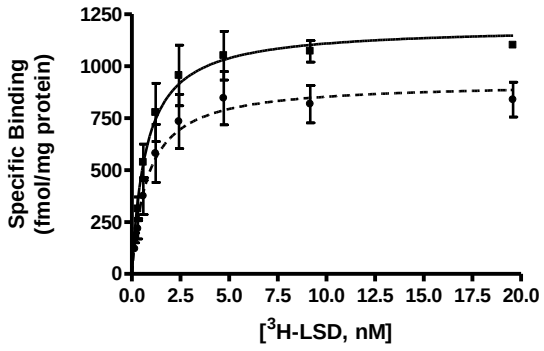

Fig. 2. Saturation binding curve for [^{3}H]LSD in CHO-FA4 cells expressing h5-HT$_{2A}$ receptors. The solid line represents the control and the dashed line represents the 20 mM DTT treatment. The points represent the mean ± S.E.M (vertical bars) values of three independent experiments (n=3) performed with triplicate measurements.

Table 1

Effect of DTT on binding capacity and affinity of [^{3}H]LSD on h5-HT$_{2A}$ receptor transfected in CHO-FA4 cells. Values represent mean ± S.E.M of three independent experiments each performed in triplicate.

	Binding Saturation	
	B_{max} (fmol/mg prot)	K_d (nM)
Control	1190 ± 63.55	0.73 ± 0.14
20 mM DTT treated	921.2 ± 60.84*	0.80 ± 0.21

* indicates $P < 0.05$ treated versus control cells (Student's *t* test).

Kinetic analysis of [^{3}H]LSD binding revealed statistically significant differences in the percentage of specific binding in association experiments in which a decrease of 40.54% in cells treated with DTT was observed ($P < 0.05$, Student's t test). The association rate (k_{on}) and association half time ($t_{1/2}$) remained unaltered relative to the control (**Fig. 3A**; **Table 2**). In the dissociation experiments, no change in the dissociation rate (k_{off}) was observed. The residence times of LSD (calculated as 1/ k_{off}) were 78.3 min for control and 57.2 min for DTT-treated cells. The dissociation constant calculated from k_{off}/k_{on} ratio was similar to that observed in saturation experiments (**Fig. 3B**; **Table 2**).

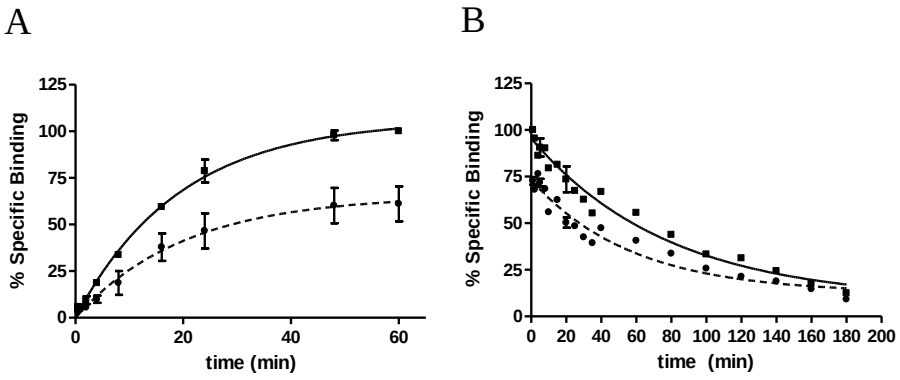

Fig. 3. Specific binding of [^{3}H]LSD to the h5-HT$_{2A}$ receptor in membranes of CHO 5-HT$_{2A}$ cells, measured in association (A) or dissociation assays (B). Non-specific binding was evaluated in presence of 1 µM methysergide. The points represent the mean ± S.E.M (vertical bars) of three independent experiments (n=3) performed with triplicate measurements.

Table 2

Kinetic parameters for [^{3}H]LSD binding to h5-HT$_{2A}$ receptor at 37 ºC. Values represent the mean of three independent experiments each performed in triplicate.

	Binding Kinetics					
	% Specific Binding (association assays)	k_{on} ($nM^{-1}min^{-1}$)	$t_{1/2}$ association (min)	k_{off} (min^{-1})	$t_{1/2}$ dissociation (min)	K_d calculated (k_{off}/k_{on}, nM)
Control	106.2 ± 2.51	0.033	14.00	0.01277	54.26	0.382
20 mM DTT treated	65.66 ± 5.77*	0.027	14.89	0.01748	39.65	0.639

* indicates $P < 0.05$ treated versus control cells (Student's t test).

In order to test the effects of DTT on antagonist binding, we carried out competition binding assays with clozapine and [^{3}H]LSD as a radioligand in membranes of CHO-5-HT$_{2A}$ cells treated or not treated with 20 mM DTT. Total specific binding decreased by 29.39 % for cells treated with DTT (P < 0.001, Student's t test), but clozapine affinity (K_i) did not change relative to untreated cells (**Fig. 4**; **Table 3**)

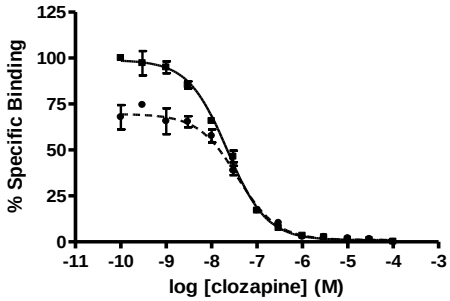

Fig. 4. [^{3}H]LSD binding displacement curves for clozapine at h5-HT$_{2A}$ receptors. The solid line represents the control and the dashed line represent cells treated with 20 mM DTT. The points represent the mean ± S.E.M (vertical bars) of four independent experiments (n=4) performed with duplicate measurements.

Table 3

Effect of DTT on competition parameters of clozapine at h5-HT$_{2A}$ receptors. The values represent the mean ± S.E.M of at least four independent experiments each performed in duplicate.

	Binding Competition	
	% Specific Binding	K_i (nM)
Control	98.95 ± 1.27	11.34 ± 0.71
20 mM DTT Treated	69.56 ± 1.88***	19.11 ± 2.76

*** indicates P < 0.001 treated versus control cells (Student's t test).

3.2. Treatment with DTT modified the activation of 5-HT$_{2A}$ receptors: quantification of AA release and IP accumulation

To assess the effect of DTT on receptor functionality, concentration-response curves of 5-HT -induced IP accumulation in the absence and presence of 20 mM DTT were constructed.

When IP accumulation was measured, the 5-HT decrease by 25.36% in the maximal response (E_{max}) for cells treated with DTT (%E_{max} of 98.82 ± 2.75 for control cells and %E_{max} of 73.46

± 2.39 for 20 mM DTT-treated cells) ($P < 0.001$, Student's *t* test). No significant differences in 5-HT potency were observed (pEC_{50} of 6.25 ± 0.07 for control and pEC_{50} of 6.08 ± 0.09 for 20mM DTT treated) (**Fig. 5**).

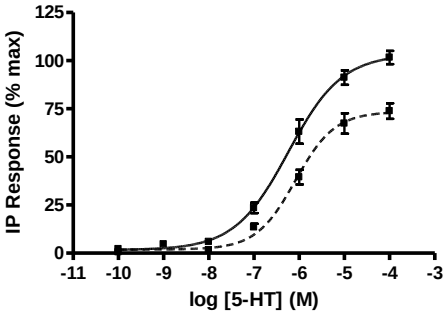

Fig. 5. Concentration-response curves of 5-HT on h5-HT_{2A} receptors induced IP accumulation. The solid line represents the control, the dashed line represents cells treated with 20 mM DTT. The points represent the mean ± S.E.M (vertical bars) of three independent experiments (*n*=3) performed with triplicate measurements.

Clozapine concentration-response curves were then constructed for the absence and presence of different concentrations of DTT (5, 20 and 40 mM). We previously observed that clozapine differentially modulates phospholipase A_2 and phospholipase C pathways coupled to human 5-HT_{2A} receptors: it inhibits 5-HT-induced stimulation of the PLA_2 pathway with a biphasic profile, while it inhibits the PLC pathway with a monophasic profile [18, 20]. DTT treatment induced a statistically significant decrease of 1 μM 5-HT-induced activation in the two signalling pathways studied ($P < 0.001$, Student's *t* test) (**Fig. 6**; **Table 4** and **Table 5**), but no significant differences in the pIC_{50} values for either signalling pathway were observed relative to the control.

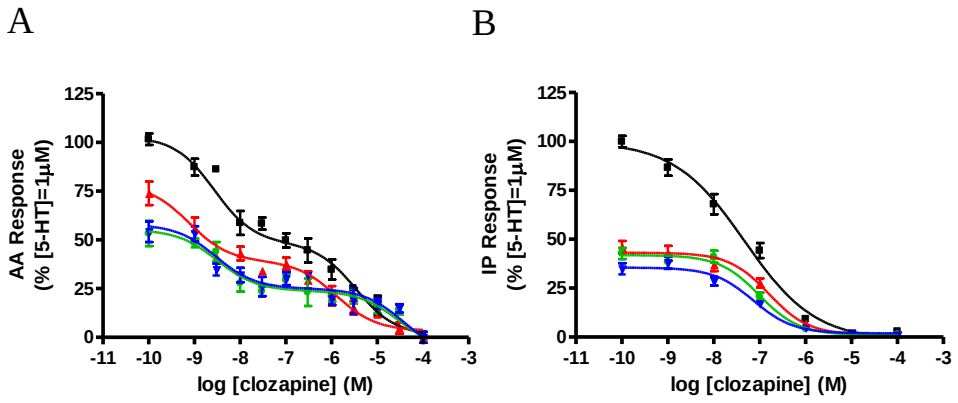

Fig. 6. (A) Concentration-response curves for clozapine on h5-HT_{2A} receptors stimulated with 1 μM 5-HT and measurement of AA release. (B) Concentration-response curves for clozapine on h5-HT_{2A} receptors stimulated with 1 μM 5-HT and measurement of IP accumulation. The black lines represent the control, the red lines represent cells treated with 5 mM DTT, the green lines represent cells treated with 20 mM DTT and the blue lines represent cells treated with 40 mM DTT. Points represent mean ± S.E.M (vertical bars) of independent experiments performed with triplicate measurements, *n*=7 for AA release and *n*=13 for IP accumulation.

Table 4

Effect of DTT on clozapine potency (pIC_{50}) and percentage of the effect elicited by 1 μM 5-HT in cells expressing human 5-HT_{2A} receptors for AA release. Values represent mean ± S.E.M of at least seven independent experiments each performed in triplicate.

	AA release	
	pIC_{50}	% E_{max} (1 μM 5-HT)
Control	8.56 ± 0.21 High; 5.46 ± 0.21 Low	103.10 ± 5.23
5 mM DTT treated	9.11 ± 0.27 High; 5.88 ± 0.22 Low	78.37 ± 6.67***
20 mM DTT treated	8.50 ± 0.23 High; 4.53 ± 0.37 Low	55.29 ± 3.81***
40 mM DTT treated	8.53 ± 0.24 High; 4.43 ± 0.40 Low	57.97 ± 4.44***

*** indicates $P < 0.001$ for treated versus control cells (Student's *t* test).

Table 5

Effect of DTT on clozapine potency (pIC_{50}) and percentage of the effect elicited by 1 μM 5-HT in cells expressing human 5-HT_{2A} receptors for IP accumulation. Values represent mean ± S.E.M of at least thirteen independent experiments each performed in triplicate.

	IPs accumulation	
	pIC_{50}	% E_{max} (1 μM 5-HT)
Control	7.32 ± 0.10	99.87 ± 4.07
5 mM DTT treated	6.80 ± 0.11	43.11 ± 1.50***
20 mM DTT treated	7.00 ± 0.10	41.88 ± 1.39***
40 mM DTT treated	7.13 ± 0.11	35.52 ± 1.29***

*** indicates $P < 0.001$ for treated versus control cells (Student's *t* test).

3.3. Treatment with DTT did not disrupt 5-HT$_{2A}$ homodimers

To test the possible involvement of disulfide bonds in 5-HT$_{2A}$ dimerization, we used BRET saturation assays to examine the effect of the reducing agent DTT on 5-HT$_{2A}$ dimerization. HEK293T cells were co-transfected with a constant amount of RLuc-N2-5-HT$_{2A}$ donor plasmid and increasing amounts of pcDNA3-5-HT$_{2A}$-YFP acceptor plasmid and they were treated or not treated (control) with DTT prior to determination of BRET efficacy. The results showed an increase in BRET signals as a function of increasing acceptor/donor expression in control cells that could be fitted to a rectangular hyperbolic function (**Fig. 7**). Neither the amplitude nor the shape of the BRET saturation curves were affected by DTT treatment (**Fig. 7**). The experiments performed yielded BRET$_{max}$ and BRET$_{50}$ values for the DTT-treated cells (mean ± S.E.M., n = 4) of 96.30 ± 4.086% and 110.0 ± 9.134 % of the values obtained for untreated cells, resulting in no statistically significant differences between both conditions (P = 0.4683 for BRET$_{max}$ and P = 0.2689 for BRET$_{50}$, Paired *t* test). This suggests that the possible effects of DTT on the integrity of cysteine-bonds do not alter the homodimerization state of the 5-HT$_{2A}$ receptors in the transfected cells.

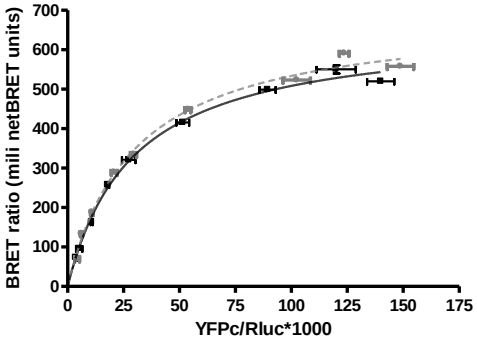

Fig. 7. BRET saturation curves for human 5-HT$_{2A}$ receptors in transfected HEK293T cells. Cells were co-transfected with a fixed amount of RLuc-N2-5-HT$_{2A}$ and increasing amounts of pcDNA3-5-HT$_{2A}$-YFP. The solid line represents untreated cells and the dashed line represents cells treated with 20 mM DTT. The graph shows the results (expressed as mean ± S.E.M.) of one representative experiment out of four, performed in quadruplicate. The R^2 values for the fitting were 0.9952 and 0.9924 for untreated and treated cells, respectively. BRET$_{max}$ values (mean ± S.E.M.) were 656.6 ± 17.18 and 691.6 ± 21.70, and BRET$_{50}$ values (mean ± S.E.M.) were 29.15 ± 2.271 and 29.59 ± 2.804, for untreated and treated cells, respectively.

3.4. In silico structural model of ECL-2 binding to the 5-HT$_{2A}$ receptor before and after DTT treatment

In order to analyze how DTT treatment may affect the structural integrity of the 5-HT$_{2A}$ receptor binding site, we performed a structural analysis of the changes in conformational freedom of ECL-2 before and after DTT treatment. To do so, we started from a model of the 5-HT$_{2A}$ receptor (see Methods). Using this structure, the ECL-2 region of two different receptor systems was subjected to a Low Mode Analysis with MOE software. In the first, the cysteine bond between ECL-2 and helix 3 was preserved (as found in untreated receptors). In the second, the bond was broken, thus mimicking the effects of DTT. As we can see in the top view of both receptor conditions in **Figure 8**, these result in different populations of ECL-2 conformations. In **Figure 8A**, we see how in the untreated receptor (with an integer cysteine bond, in yellow vdW representation) ECL-2 is more constrained to the extracellular region. This ECL-2 constraint seems to be important for maintaining an open binding pocket that can accommodate an orthosteric ligand (e.g. LSD, orange VdW, see **Fig. 8C**). Conversely, in the receptor with a broken cysteine bond (yellow vdW representation, **Fig. 8B**) ECL-2 adopts a wider variety of conformations. Some of these conformations protrude deeper into the receptor orthosteric binding pocket leading to collapse of the pocket. A shrunken binding pocket would be incapable of accommodating LSD (orange VdW, **Fig. 8D**) due to a large degree of overlap of ECL-2 with the orthosteric ligand. These observations are consistent with the lower availability of LSD binding sites observed in our experiments.

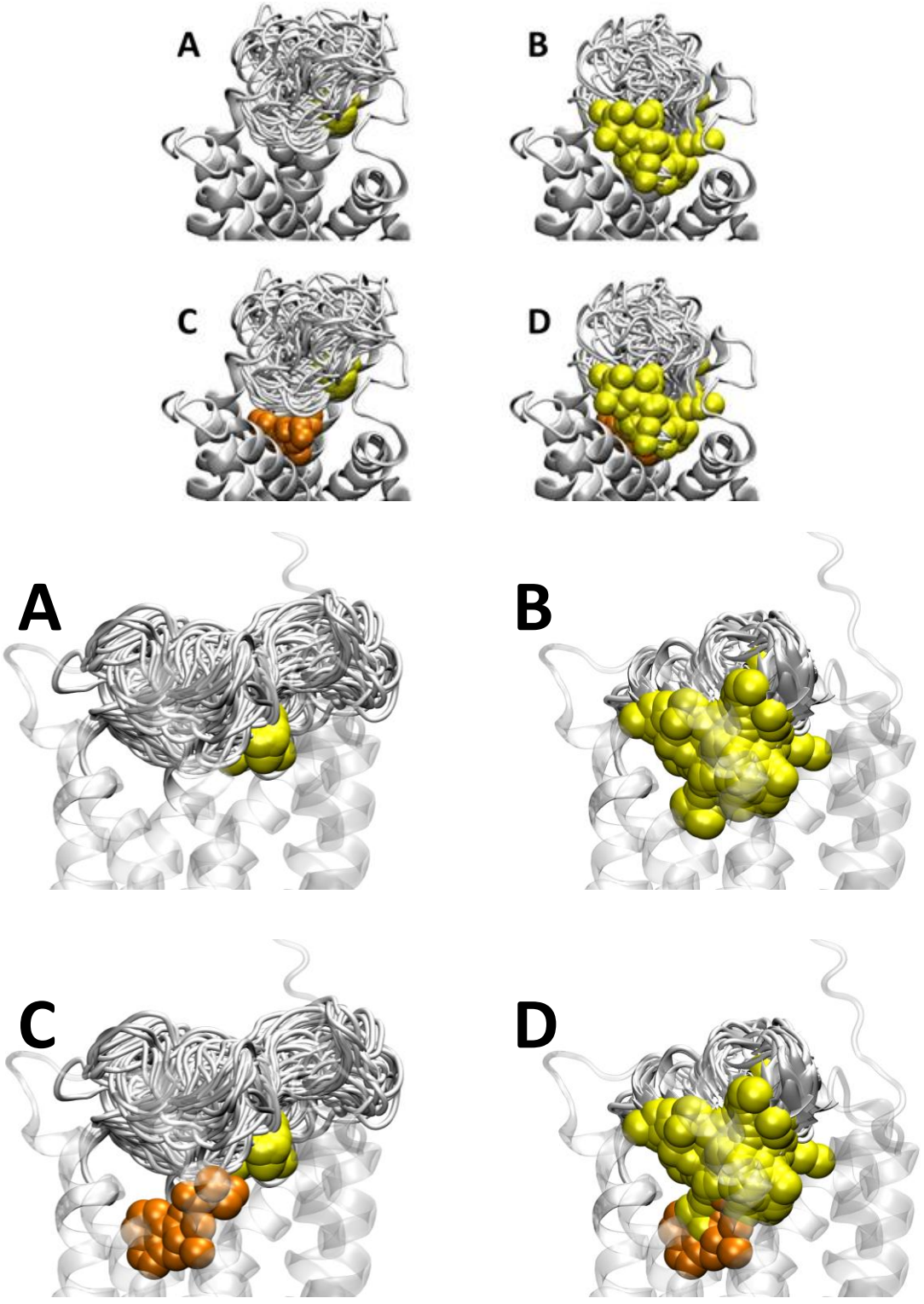

Fig. 8. Conformational analysis of ECL-2. ECL conformational freedom was assessed before (A) and after (B) cysteine bond cleavage. In both representations we can see different conformational states of each receptor condition. The two cysteine residues originally forming the bond are shown in yellow. In order to assess how this different conformational freedom may affect LSD binding, the binding mode of the ligand was assessed. The superimposed structure of LSD to the receptor before (C) and after (D) cysteine cleavage is represented in orange.

4. Discussion

The major finding of this study was that rupture of the disulfide bridge in the 5-HT_{2A} receptor with the reducing agent DTT alters its binding and activation properties by disturbing its conformation without changing its dimeric structure.

The 5-HT_{2A} receptor has been reported to establish an extracellular conserved disulfide bridge between Cys^{148} in the TM3 and Cys^{227} located in the ECL-2. In addition to the two cysteines involved in the conserved disulfide bridge, the 5-HT_{2A} receptor has another six cysteines that could form other disulfide bridges. However, as the crystal structure is not known, the existence of other disulfide bonds in the extracellular face cannot be determined. Other additional disulfide bonds between ECL-2 and N-terminus, ECL-3 and N-terminus or intra ECL-2 have been described for other receptors and in some cases the conserved disulfide bridge is not present and another intra ECL-2 or intra ECL-3 is present [8].

The disulfide bond reducing agent DTT was used to investigate the effects of disulfide reduction of various membrane receptors, with the extracellular receptor surface being the most exposed and accessible to reducing agents. Numerous experiments have shown that treatment with DTT causes a decrease in the ligand binding on β-adrenergic receptors [27-29], D_2 receptors [30], 5-HT_{1A} receptors [31] and prostacyclin receptors [32], among others. However, an increase in ligand binding or activation has also been observed in other receptors. Some examples are the histamine H_1 receptor [33-37], β-adrenergic receptors [38] and N-methyl-D-aspartate (NMDA) receptors [39, 40].

Here, we hypothesized that the disulfide bridge between Cys^{148} (TM3) and Cys^{227} (ECL-2) may determine ligand recognition and receptor activation due to the rigidity that it provides to the 5-HT_{2A} receptor by anchoring the extracellular side of the helix near the binding site and limiting the extent of the conformational changes in this region. To study this hypothesis, we analyzed ligand binding and the function of the 5-HT_{2A} receptor after treatment with the

reducing agent DTT. We used [^{3}H]LSD, a hallucinogenic agonist, in radioligand assays in order to stabilize the active conformations at 5-HT_{2A} receptors. DTT treatment induced a statistically significant decrease in B_{max} values and in the percentage of specific binding in saturation and association experiments with [^{3}H]LSD, but without affecting radioligand affinity (K_d). The observed decrease in LSD residence time on DTT-treated cells is consistent with the previously described mutation in ECL-2 (L229A) in 5-HT_{2A} receptor, because the flexibility of the lid increases [22]. Furthermore, DTT treatment induced a significant decrease in the percentage of specific binding without any change in clozapine K_i values in competition assays (11.34 ± 0.71 nM for control and 19.11 ± 2.76 nM for DTT treatment). These results suggest that DTT treatment disrupts disulfide bridges, thereby reducing the number of available [^{3}H]LSD binding sites (lower B_{max}) without modifying the affinity of ligands. According to the *in silico* study, the reduced number of binding sites may be the result of the collapse of the binding pocket caused by destruction of the disulfide bridge.

Similar effects on receptor pharmacology have been observed for the β-adrenergic receptor, with a decrease in B_{max} for DTT treated receptors without any effect on the affinity of [^{3}H]dihydroalprenolol [29]. However, other studies showed that DTT treatment induced a decrease in K_d values and B_{max} [27, 30, 41-43]. The findings of both studies explained the results obtained based on the reduction of a disulfide bridge in the receptor that is important for ligand binding, either by direct participation in ligand recognition or its proximity to the binding site. It has also been observed that incubation of the ligand before DTT treatment protects the receptor from the reducing effect of DTT due to a conformational change, so that ligand occupancy masks the structurally critical disulfide bridge due to its proximity to the ligand binding pocket.

In a further step, we studied DTT-induced modulation of receptor signalling. We first evaluated the effect of DTT treatment in 5-HT-mediated PLC pathway activation by

determining concentration-response curves in the absence and presence of 20 mM DTT. The results showed a statistically significant decrease in E_{max} of IP accumulation in the presence of DTT, although the potency values were unchanged.

Given that clozapine shows functional selectivity with a combination of biphasic and monophasic inhibition curves in both binding and functional assays measuring AA and IP release [19], we constructed concentration-response curves for clozapine in the absence and presence of different concentrations of DTT. This allowed us to evaluate the effect of breaking disulfide bridges in signalling through both PLA_2 and PLC pathways. The results showed a statistically significant decrease in 5-HT E_{max} in both pathways, although the clozapine inhibition profiles observed in treated cells were the same relative to the control. The curves were the same in both untreated and DTT-treated receptors (monophasic in the PLC pathway and biphasic in the PLA_2 pathway) and potency values were unchanged.

Similar results were found in rat forebrain synaptoneurosomes, in which DTT also produced dose-dependent inhibition of IP accumulation produced by glutamate and potassium in the metabotropic glutamate receptor [44]. In the human prostacyclin receptor, a decrease in cAMP production was also observed when β-mercaptoethanol (β-ME) was used as the reducing agent, with no effect on the EC_{50} value. In the same study, competition experiments carried out in the presence of β-ME or DTT showed a decrease in [^{3}H]iloprost specific binding without any change in affinity [32].

According to the results of our functional experiments, the dimeric structure of 5-HT_{2A} receptors was conserved after DTT treatment. However, western-blot experiments have shown that DTT treatment also causes the rupture of GPCR dimers on different receptors [45-50]. In order to clarify this question, BRET experiments were carried out to confirm the preservation of the dimeric structure of these receptors. As expected, DTT treatment did not modify the BRET signal, suggesting that breakage of disulfide bridges did not disrupt the

dimer (either because the disulfide bridges do not contribute to the dimerization interface or because of the presence of other protein-protein interactions stabilizing the dimer). Nevertheless, the binding and functional results suggest that, after DTT treatment, the TM3-ECL-2 disulfide bridge is disrupted, thus allowing the receptor to adopt different conformations. This is consistent with results reported by Lin and colleagues [51], who studied the structural changes of β_2-adrenergic receptor in response to DTT treatment by circular dichroism (CD) spectroscopy and intrinsic tryptophan fluorescence experiments. In CD experiments, these authors showed that the secondary structure of the receptor had not been disturbed after treatment, but tryptophan fluorescence spectra demonstrated that DTT induced a reversible conformational change in the tertiary structure of β_2-receptor [51].

Extracellular loops are known to play important functional roles in ligand binding and receptor activation [2-4, 52-59]. The second extracellular loop in class A GPCRs is the longest and most divergent of the three as it can differ greatly in length and in sequence [60]. Recently reported crystal structures show that the conserved disulfide bridge forces ECL-2 to form a lid over the binding pocket, and that ECL-2 contains well defined but rather different secondary structures within the different receptor families [55, 61-64]. It has also been speculated that the ECL-2 adopts different conformations during ligand binding and receptor activation, first allowing the ligand to enter the binding pocket (open conformation) and secondly stabilizing ligand-stabilized receptor conformations (closed over the ligand). The ECL-2 thus functions as a gatekeeper for entry into the orthosteric binding site and the flexibility and conformational integrity of ECL-2 are also important. Moreover, ECL-2 is also known to be associated with ligand selectivity by adopting distinct conformations on empty receptor or bound ligand and interacting differently between agonists (total or partial), inverse agonists or antagonists [65, 66]. For instance, in the adenosine A_{2A} receptor, ECL-2 may also be an important determinant in the subtype selectivity of ligands [67]. The correct orientation

of the ECL-2 is thus restrained by the conserved disulfide bond and plays an important role in producing different functional states of the receptor. In addition, the involvement of ECL-2 in biased agonism has been shown in class-B and class-A GPCRs [68, 69]. Disruption of the conserved disulfide bridge interferes with the receptor conformation and this could shift the equilibrium of active/inactive receptor populations in any direction.

Furthermore, in 5-HT_{2A} and 5-HT_{2B} receptors a decrease in E_{max} was observed in the β-arrestin pathway when L229A and L209A were mutated, but not in PLC pathway [22]. Our results complement the findings of the aforementioned study by showing that the disulfide bridge is disrupted without modifying the primary structure of 5-HT_{2A} receptor. A decrease in E_{max} was thus also obtained in PLA_2 and PLC pathways, suggesting a role for the disulfide bridge in ligand binding and activation.

In summary, our results show that the disulfide bridge between TM3 and ECL-2 is essential for 5-HT_{2A} receptor signalling in both PLA_2 and PLC pathways, but not for the homodimeric nature of these receptors. This reveals the integrity of the ECL-2 epitope, which should be explored for developing novel ligands acting as allosteric modulators of 5-HT_{2A} receptors.

Acknowledgments

This work was supported by Ministerio de Ciencia e Innovacion (SAF2009-13609-C04-01), Ministerio de Economia y Competitividad (SAF2014-57138-C2-2R), and Innopharma project (PI12/00742; Ministerio de Economía y Competitividad -FEDER). A.I. was recipient of a FPI fellowship from Ministerio de Ciencia e Innovacion. M. Cimadevila is recipient of a financial support from the Xunta de Galicia and the European Union (European Social Fund - ESF).

Conflict of interest

The authors declare no conflicts of interest.

References

[1] Venkatakrishnan AJ, Deupi X, Lebon G, Tate CG, Schertler GF, Babu MM (2013). Molecular signatures of G-protein-coupled receptors. Nature. 494: 185-194.

[2] Wheatley M, Wootten D, Conner MT, Simms J, Kendrick R, Logan RT *et al.* (2012). Lifting the lid on GPCRs: the role of extracellular loops. Br. J. Pharmacol. 165: 1688-1703.

[3] Wheatley M, Simms J, Hawtin SR, Wesley VJ, Wooten D, Conner M *et al.* (2007). Extracellular loops and ligand binding to a subfamily of Family A G-protein-coupled receptors. Biochem. Soc. Trans. 35: 717-720.

[4] Kclo JM, Wiegand CB, Narzinski K, Baranski TJ (2005). Essential role for the second extracellular loop in C5a receptor activation. Nat. Struct. Mol. Biol. 12: 320-326.

[5] Park PS, Filipek S, Wells JW, Palczewski K (2004). Oligomerization of G protein-coupled receptors: past, present, and future. Biochemistry. 43: 15643-15656.

[6] Angers S, Salahpour A, Bouvier M (2002). Dimerization: an emerging concept for G protein-coupled receptor ontogeny and function. Annu. Rev. Pharmacol. Toxicol. 42: 409-435.

[7] Rios CD, Jordan BA, Gomes I, Devi LA (2001). G-protein-coupled receptor dimerization: modulation of receptor function. Pharmacol. Ther. 92: 71-87.

[8] Storjohann L, Holst B, Schwartz TW (2008). A second disulfide bridge from the N-terminal domain to extracellular loop 2 dampens receptor activity in GPR39. Biochemistry. 47: 9198-9207.

[9] Vaidehi N, Kenakin T (2010). The role of conformational ensembles of seven transmembrane receptors in functional selectivity. Curr. Opin. Pharmacol. 10: 775-781.

[10] Kenakin T (1995). Agonist-receptor efficacy I: Mechanisms of efficacy and receptor promiscuity. Trends. Pharmacol. Sci. 16: 188-192.

[11] Jarpe MB, Knall C, Mitchell FM, Buhl AM, Duzic E, Johnson GL (1998). [D-Arg1,D-Phe5,D-Trp7,9,Leu11] Substance P acts as a biased agonist toward neuropeptide and chemokine receptors. J. Bio. Chem. 273: 3097-3104.

[12] Urban JD, Clarke WP, von Zastrow M, Nichols DE, Kobilka B, Weinstein H *et al.* (2007). Functional selectivity and classical concepts of quantitative pharmacology. J. Pharmacol. Exp. Ther. 320: 1-13.

[13] Kenakin T (2007). Collateral efficacy in drug discovery: taking advantage of the good (allosteric) nature of 7TM receptors. Trends. Pharmacol. Sci. 28: 407-415.

[14] González-Maeso J, Ang RL, Yuen T, Chan P, Weisstaub NV, López-Giménez JF *et al*. (2008). Identification of a serotonin/glutamate receptor complex implicated in psychosis. Nature. 452: 93-97.

[15] Roth BL, Willins DL, Kristiansen K, Kroeze WK (1998). 5-Hydroxytryptamine2-family receptors (5-hydroxytryptamine2A, 5-hydroxytryptamine2B, 5-hydroxytryptamine2C): where structure meets function. Pharmacol. Ther. 79: 231-257.

[16] Berg KA, Maayani S, Goldfarb J, Scaramellini C, Leff P, Clarke WP (1998). Effector pathway-dependent relative efficacy at serotonin type 2A and 2C receptors: evidence for agonist-directed trafficking of receptor stimulus. Mol. Pharmacol. 54: 94-104.

[17] Hoyer D, Clarke DE, Fozard JR *et al*. (1994). International Union of Pharmacology classification of receptors for 5-hydroxytryptamine (Serotonin). Pharmacol. Rev. 46: 157-203.

[18] Felder CC, Kanterman RY, Ma AL, Axelrod J (1990). Serotonin stimulates phospholipase A2 and the release of arachidonic acid in hippocampal neurons by a type 2 serotonin receptor that is independent of inositolphospholipid hydrolysis. Proc. Natl. Acad. Sci. USA. 87: 2187-2191.

[19] Brea J, Castro M, Giraldo J, Lopez-Gimenez JF, Padín JF, Quntián F *et al*. (2009). Evidence for distinct antagonist-revealed functional states of 5-hydroxytryptamine2A receptor homodimers. Mol. Pharmacol. 75: 1380-1391.

[20] Albizu L, Balestre MN, Breton C, Pin JP, Manning M, Mouillac B *et al*. (2006). Probing the existence of G protein-coupled receptor dimers by positive and negative ligand-dependent cooperative binding. Mol. Pharmacol. 70: 1783-1791.

[21] Iglesias A, Lage S, Cadavid MI, Loza MI, Brea J (2016). Development of a multiplex assay for studying functional selectivity of human serotonin 5-HT2A receptors and identification of active compounds by high throughput screening. J. Biomol. Screen. 21: 816-823.

[22] Wacker D, Wang S, McCorvy JD, Betz RM, Venkatakrishnan AJ, Levit A *et al*. (2017). Crystal structure of an LSD-bound human serotonin receptor. Cell. 168: 377-389.

[23] Jenkins L, Brea J, Smith NJ, Hudson BD, Reilly G, Bryant NJ *et al.* (2010). Identification of novel species-selective agonists of the G-protein-coupled receptor GPR35 that promote recruitment of B-arrestin-2 and activate Gα13. Biochem. J. 432: 451-459.

[24] Case DA, Darden TA , Cheatham TE, III, Simmerling CL, Wang J *et al.* (2012). AMBER 12, University of California, San Francisco.

[25] Laskowski RA, MacArthur MW, Moss DS, Thornton JM (1993). PROCHECK: A program to check the stereochemical quality of protein structures. J. Appl. Crystallogr. 26: 283–291.

[26] Giraldo J, Vivas NM, Vila E, Badia A (2002). Assessing the (a)symmetry of concentration-effect curves: empirical versus mechanistic models. Pharmacol. Ther. 95: 21-45.

[27] Noda K, Saad Y, Graham RM, Karnik SS (1994). The high affinity state of the beta 2-adrenergic receptor requires unique interaction between conserved and non-conserved extracellular loop cysteines. J. Biol. Chem. 269: 6743-6752.

[28] Dohlman HG, Caron MG, DeBlasi A, Frielle T, Lefkowitz RJ (1990). Role of extracellular disulfide-bonded cysteines in the ligand binding function of the beta 2-adrenergic receptor. Biochemistry. 29: 2335-2342.

[29] Vauquelin G, Bottari S, Kanarek L, Strosberg AD (1979). Evidence for essential disulfide bonds in beta1-adrenergic receptors of turkey erythrocyte membranes. Inactivation by dithiothreitol. J. Biol. Chem. 254: 4462-4469.

[30] Reader TA, Molina-Holgado E, Lima L, Boulianne S, Dewar KM (1992). Specific [3H]raclopride binding to neostriatal dopamine D2 receptors: role of disulfide and sulfhydryls groups. Neurochem. Res. 17: 749-759.

[31] Harikumar KG, John PT, Chattopadhyay A (2000). Role of disulfides and sulfhydryl groups in agonist and antagonist binding in serotonin1A receptors from bovine hippocampus. Cell. Mol. Neurobiol. 20: 665-681.

[32] Stitham J, Gleim SR, Douville K, Arehart E, Hwa J (2006). Versatility and differential roles of cysteine residues in human prostacyclin receptor structure and function. J. Biol. Chem. 281: 37227-37236.

[33] Dickenson JM, Hill SJ (1994). Selective potentiation of histamine H1-receptor stimulated calcium responses by 1,4-dithiothreitol in DDT1MF-2 cells. Biochem. Pharmacol. 48: 1721-1728.

[34] Carman-Krzan M (1984). The effect of group selective reagents N-ethylmaleimide and dithiothreitol on histamine H1-receptor binding sites in the vascular smooth muscle membranes. Agents Actions. 14: 561-565.

[35] Donaldson J, Hill SJ (1986a). Selective enhancement of histamine H1-receptor responses in guinea-pig ileal smooth muscle by 1,4-dithiothreitol. Br. J. Pharmacol. 87: 191-199.

[36] Donaldson J, Hill SJ (1986b). 1,4-Dithiothreitol-induced alteration in histamine H1-agonist binding in guinea-pig cerebellum and cerebral cortex. Eur. J. Pharmacol. 129: 25-31.

[37] Donaldson J, Hill SJ (1986c). Enhancement of histamine H1-receptor agonist activity by 1,4-dithiothreitol in guinea-pig cerebellum and cerebral cortex. J. Neurochem. 47: 1476-1482.

[38] Pedersen SE, Ross EM (1985). Functional activation of beta-adrenergic receptors by thiols in the presence or absence of agonists. J. Biol. Chem. 260: 14150-14157.

[39] Talukder I, Kazi R, Wollmuth LP (2011). GluN1-specific redox effects on the kinetic mechanism of NMDA receptor activation. Biophys. J. 101: 2389-2398.

[40] Reynolds IJ, Rush EA, Aizenman E (1990). Reduction of NMDA receptors with dithiothreitol increases [3H]-MK-801 binding and NMDA-induced Ca^{2+} fluxes. Br. J. Pharmacol. 101: 178-182.

[41] Dorn GW 2nd (1990). Cyclic oxidation-reduction reactions regulate thromboxane A2/prostaglandin H2 receptor number and affinity in human platelet membranes. J. Biol. Chem. 265: 4240-4246.

[42] Huang M, Rorstad OP (1989). Effects of GTP analogs and dithiothreitol on the binding properties of the vascular vasoactive intestinal peptide receptor. Can. J. Physiol. Pharmacol. 67: 851-856.

[43] Wright M, Drummond GI (1983). Inactivation of the beta-adrenergic receptor in skeletal muscle by dithiols. Biochem. Pharmacol. 32: 509-515.

[44] Vignes M, Guiramand J, Sassetti I, Recasens M (1992). Dithiotreitol specifically inhibits metabotropic responses of glutamate and depolarizing agents in rat brain synaptoneurosomes. Neurochem. Int. 21: 229-235.

[45] Fay JF, Farrens DL (2013). The membrane proximal region of the cannabinoid receptor CB1 N-terminus can allosterically modulate ligand binding affinity. Biochemistry. 52: 8286-8294.

[46] Berthouze M, Rivail L, Lucas A, Ayoub MA, Russo O, Sicsic S *et al.* (2007). Two transmembrane Cys residues are involved in 5-HT4 receptor dimerization. Biochem. Biophys. Res. Commun. 356: 642-647.

[47] Michineau S, Alhenc-Gelas F, Rajerison RM (2006). Human bradykinin B2 receptor sialylation and N-glycosylation participate with disulfide bonding in surface receptor dimerization. Biochemistry. 45: 2699-2707.

[48] Zeng F, Wess J (2000). Molecular aspects of muscarinic receptor dimerization. Neuropsychopharmacology. 23: S19-S31.

[49] Zeng FY, Soldner A, Schöneberg T, Wess J (1999). Conserved extracellular cysteine pair in the M3 muscarinic acetylcholine receptor is essential for proper receptor cell surface localization but not for G protein coupling. J. Neurochem. 72: 2404-2414.

[50] Romano C, Yang WL, O'Malley KL (1996). Metabotropic glutamate receptor 5 is a disulfide-linked dimer. J. Biol. Chem. 271: 28612-28616.

[51] Lin S, Gether U, Kobilka BK. Ligand stabilization of the beta 2 adrenergic receptor: effect of DTT on receptor conformation and fluorescence monitored by circular dichroism spectroscopy. Biochemistry. 35: 14445-14451.

[52] Avlani VA, Gregory KJ, Morton CJ, Parker MW, Sexton PM, Christopoulos A (2007). Critical role for the second extracellular loop in the binding of both orthosteric and allosteric G protein-coupled receptor ligands. J. Biol. Chem. 282: 25677-25686.

[53] Conner M, Hawtin SR, Simms J, Wootten D, Lawson Z, Conner AC, Parslow RA,and Wheatley M (2007). Systematic analysis of the entire second extracellular loopof the V(1a)

vasopressin receptor: key residues, conserved throughout a G-protein coupled receptor family, identified. .J Biol. Chem. 282:17405–17412.

[54] Scarselli M, Li B, Kim SK, Wess J (2007). Multiple residues in the second extracellular loop are critical for M3 muscarinic acetylcholine receptor activation. J. Biol. Chem. 282: 7385-7396.

[55] Palczewski K, Kumasaka T, Hori T, Behnke CA, Motoshima H, Fox BA *et al*. (2000). Crystal structure of rhodopsin: A G protein-coupled receptor. Science. 289: 739-745.

[56] Barington L, Rummel PC, Lückmann M, Pihl H, Larsen O, Daugvilaite V *et al*. (2016). Role of conserved disulfide bridges and aromatic residues in extracellular loop 2 of chemokine receptor CCR8 for chemokine and small molecule binding. J. Biol. Chem. 291: 16208-16220.

[57] Nguyen AT, Baltos JA, Thomas T, Nguyen TD, Muñoz LL, Gregory KJ *et al.* (2016). Extracellular loop 2 of the adenosine A1 receptor has a key role in orthosteric ligand affinity and agonist efficacy. Mol. Pharmacol. 90: 703-714.

[58] Nguyen AT, Vecchio EA, Thomas T, Nguyen TD, Aurelio L, Scammells PJ *et al*. (2016). Role of the second extracellular loop of the adenosine A1 receptor on allosteric modulator binding, signaling, and cooperativity. Mol. Pharmacol. 90: 715-725.

[59] Ragnarsson L, Andersson Å, Thomas WG, Lewis RJ (2014). Extracellular surface residues of the α1B-adrenoceptor critical for G protein-coupled receptor function. Mol. Pharmacol. 87:121-129.

[60] Peeters MC, van Westen GJ, Li Q, IJzerman AP (2011). Importance of the extracellular loops in G protein-coupled receptors for ligand recognition and receptor activation. Trends. Pharmacol. Sci. 32: 35-42.

[61] Shimamura T, Shiroishi M, Weyand S, Tsujimoto H, Winter G, Katritch V *et al*. (2011). Structure of the human histamine H1 receptor complex with doxepin. Nature. 475: 65-70.

[62] Warne T, Serrano-Vega MJ, Baker JG, Moukhametzianov R, Edwards PC, Henderson R *et al.* (2008). Structure of a beta1-adrenergic G-protein-coupled receptor. Nature. 454: 486-491.

[63] Rasmussen SG, Choi HJ, Rosenbaum DM, Kobilka TS, Thian FS, Edwards PC *et al.* (2007). Crystal structure of the human β2 adrenergic G-protein-coupled receptor. Nature. 450: 383-387.

[64] Shi L, Javitch JA (2004). The second extracellular loop of the dopamine D2 receptor lines the binding-site crevice. Proc. Natl. Acad. Sci. U S A. 101:440-445.

[65] Unal H, Jagannathan R, Bhat MB, Karnik SS (2010). Ligand-specific conformation of extracellular loop-2 in the angiotensin II type 1 receptor. J Biol Chem. 285: 16341-16350.

[66] Banères JL, Mesnier D, Martin A, Joubert L, Dumuis A, Bockaert J (2005). Molecular characterization of a purified 5-HT4 receptor: a structural basis for drug efficacy. J. Biol. Chem. 280: 20253-20260.

[67] de Zwart M, Vollinga RC, Beukers MW, Sleegers DF, von Fritag JK, Künzel D *et al.* (1999). Potent antagonists for the human adenosine A(2B) receptor. Derivatives of the triazolotriazine adenosine receptor antagonist ZM241385 with high affinity. Drug. Dev. Res. 48: 95-103.

[68] Wootten D, Reynolds CA, Smith KJ, Mobarec JC, Koole C, Savage EE *et al.* (2016). The extracellular surface of the GLP-1 receptor is a molecular trigger for biased agonism. Cell. 165: 1632-1643.

[69] Soto AG, Smith TH, Chen B, Bhattacharya S, Cordova IC, Kenakin T *et al.* (2015). N-linked glycosylation of protease-activated receptor-1 at extracellular loop 2 regulates G-protein signaling bias. Proc. Natl. Acad. Sci. USA. 112: E3600-E3608.

Tables and table legends

Table 1

Effect of DTT on binding capacity and affinity of [^{3}H]LSD on h5-HT$_{2A}$ receptor transfected in CHO-FA4 cells. Values represent mean ± S.E.M of three independent experiments each performed in triplicate.

	Binding Saturation	
	B_{max} (fmol/mg prot)	K_d (nM)
Control	1190 ± 63.55	0.73 ± 0.14
20 mM DTT Treated	921.2 ± 60.84*	0.80 ± 0.21

* indicates $P < 0.05$ treated versus control cells (Student's *t* test)

Table 2

Kinetic parameters for [^{3}H]LSD binding to h5-HT$_{2A}$ receptor at 37 ºC. Values represent the mean of three independent experiments each performed in triplicate.

	Binding Kinetics					
	% Specific Binding (association assays)	k_{on} (nM^{-1}min^{-1})	$t_{1/2}$ association (min)	k_{off} (min^{-1})	$t_{1/2}$ dissociation (min)	K_d calculated (k_{off}/k_{on}, nM)
Control	106.2 ± 2.51	0.033	14.00	0.01277	54.26	0.382
20 mM DTT treated	65.66 ± 5.77*	0.027	14.89	0.01748	39.65	0.639

* indicates $P < 0.05$ treated versus control cells (Student's *t* test).

Table 3

Effect of DTT on competition parameters of clozapine at h5-HT$_{2A}$ receptors. The values represent the mean ± S.E.M of at least four independent experiments each performed in duplicate.

	Binding Competition	
	% Specific Binding	K_i (nM)
Control	98.95 ± 1.27	11.34 ± 0.71
20 mM DTT treated	69.56 ± 1.88***	19.11 ± 2.76

*** indicates $P < 0.001$ treated versus control cells (Student's *t* test).

Table 4

Effect of DTT on clozapine potency (pIC_{50}) and percentage of the effect elicited by 1 μM 5-HT in cells expressing human 5-HT_{2A} receptors for AA release. Values represent mean ± S.E.M of at least seven independent experiments each performed in triplicate.

	AA release	
	pIC_{50}	% E_{max} (1 μM 5-HT)
Control	8.56 ± 0.21 High; 5.46 ± 0.21 Low	103.10 ± 5.23
5 mM DTT treated	9.11 ± 0.27 High; 5.88 ± 0.22 Low	78.37 ± 6.67***
20 mM DTT treated	8.50 ± 0.23 High; 4.53 ± 0.37 Low	55.29 ± 3.81***
40 mM DTT treated	8.53 ± 0.24 High; 4.43 ± 0.40 Low	57.97 ± 4.44***

*** indicates $P < 0.001$ for treated versus control cells (Student's *t* test).

Table 5

Effect of DTT on clozapine potency (pIC_{50}) and percentage of the effect elicited by 1 μM 5-HT in cells expressing human 5-HT_{2A} receptors for IP accumulation. Values represent mean ± S.E.M of at least thirteen independent experiments each performed in triplicate.

	IPs accumulation	
	pIC_{50}	% E_{max} (1 μM 5-HT)
Control	7.32 ± 0.10	99.87 ± 4.07
5 mM DTT treated	6.80 ± 0.11	43.11 ± 1.50***
20 mM DTT treated	7.00 ± 0.10	41.88 ± 1.39***
40 mM DTT treated	7.13 ± 0.11	35.52 ± 1.29***

*** indicates $P < 0.001$ for treated versus control cells (Student's *t* test).

Figure legends

Fig. 1. A secondary structure model of the human 5-HT_{2A} receptor. The location of 15 cysteine residues (black circles) and the conserved disulfide bridge are indicated (modified from www.gpcrdb.org).

Fig. 2. Saturation binding curve for [^{3}H]LSD in CHO-FA4 cells expressing h5-HT_{2A} receptors. The solid line represents the control and the dashed line represents the 20 mM DTT treatment. The points represent the mean ± S.E.M (vertical bars) values of three independent experiments (*n*=3) performed with triplicate measurements.

Fig. 3. Specific binding of [^{3}H]LSD to the h5-HT_{2A} receptor in membranes of CHO 5-HT_{2A} cells, measured in association (A) or dissociation assays (B). Non-specific binding was evaluated in presence of 1 μM methysergide. The points represent the mean ± S.E.M (vertical bars) of three independent experiments (*n*=3) performed with triplicate measurements.

Fig. 4. [^{3}H]LSD binding displacement curves for clozapine at h5-HT_{2A} receptors. The solid line represents the control and the dashed line represent cells treated with 20 mM DTT. The points represent the mean ± S.E.M (vertical bars) of four independent experiments (*n*=4) performed with duplicate measurements.

Fig. 5. Concentration-response curves of 5-HT on h5-HT_{2A} receptors induced IP accumulation. The solid line represents the control, the dashed line represents cells treated with 20 mM DTT. The points represent the mean ± S.E.M (vertical bars) of three independent experiments (*n*=3) performed with triplicate measurements.

Fig. 6. (A) Concentration-response curves for clozapine on h5-HT_{2A} receptors stimulated with 1 μM 5-HT and measurement of AA release. (B) Concentration-response curves for clozapine on h5-HT_{2A} receptors stimulated with 1 μM 5-HT and measurement of IP accumulation. The black lines represent the control, the red lines represent cells treated with 5 mM DTT, the

green lines represent cells treated with 20 mM DTT and the blue lines represent cells treated with 40 mM DTT. Points represent mean ± S.E.M (vertical bars) of independent experiments performed with triplicate measurements, *n*=7 for AA release and *n*=13 for IP accumulation.

Fig. 7. BRET saturation curves for human 5-HT_{2A} receptors in transfected HEK293T cells. Cells were co-transfected with a fixed amount of RLuc-N2-5-HT_{2A} and increasing amounts of pcDNA3-5-HT_{2A}-YFP. The solid line represents untreated cells and the dashed line represents cells treated with 20 mM DTT. The graph shows the results (expressed as mean ± S.E.M.) of one representative experiment out of four, performed in quadruplicate. The R^2 values for the fitting were 0.9952 and 0.9924 for untreated and treated cells, respectively. $BRET_{max}$ values (mean ± S.E.M.) were 656.6 ± 17.18 and 691.6 ± 21.70, and $BRET_{50}$ values (mean ± S.E.M.) were 29.15 ± 2.271 and 29.59 ± 2.804, for untreated and treated cells, respectively.

Fig. 8. Conformational analysis of ECL-2. ECL conformational freedom was assessed before (A) and after (B) cysteine bond cleavage. In both representations we can see different conformational states of each receptor condition. The two cysteine residues originally forming the bond are shown in yellow. In order to assess how this different conformational freedom may affect LSD binding, the binding mode of the ligand was assessed. The superimposed structure of LSD to the receptor before (C) and after (D) cysteine cleavage is represented in orange.

Table 1

Effect of DTT on binding capacity and affinity of [^{3}H]LSD on h5-HT$_{2A}$ receptor transfected in CHO-FA4 cells. Values represent mean ± S.E.M of three independent experiments each performed in triplicate.

	Binding Saturation	
	B_{max} (fmol/mg prot)	K_d (nM)
Control	1190 ± 63.55	0.73 ± 0.14
20 mM DTT Treated	921.2 ± 60.84*	0.80 ± 0.21

* indicates $P < 0.05$ treated versus control cells (Student's t test)

Table 2

Kinetic parameters for [^{3}H]LSD binding to h5-HT$_{2A}$ receptor at 37 ºC. Values represent the mean of thr each performed in triplicate.

	Binding Kinetics			
	% Specific Binding (association assays)	k_{on} ($nM^{-1}min^{-1}$)	$t_{1/2}$ association (min)	k_{off} (min^{-1})
Control	106.2 ± 2.51	0.033	14.00	0.01277
20 mM DTT treated	65.66 ± 5.77*	0.027	14.89	0.01748

* indicates $P < 0.05$ treated versus control cells (Student's t test).

Table 3

Effect of DTT on competition parameters of clozapine at h5-HT$_{2A}$ receptors. The values represent the mean ± S.E.M of at least four independent experiments each performed in duplicate.

	Binding Competition	
	% Specific Binding	K_i (nM)
Control	98.95 ± 1.27	11.34 ± 0.71
20 mM DTT treated	69.56 ± 1.88***	19.11 ± 2.76

*** indicates $P < 0.001$ treated versus control cells (Student's t test).

Figure 1

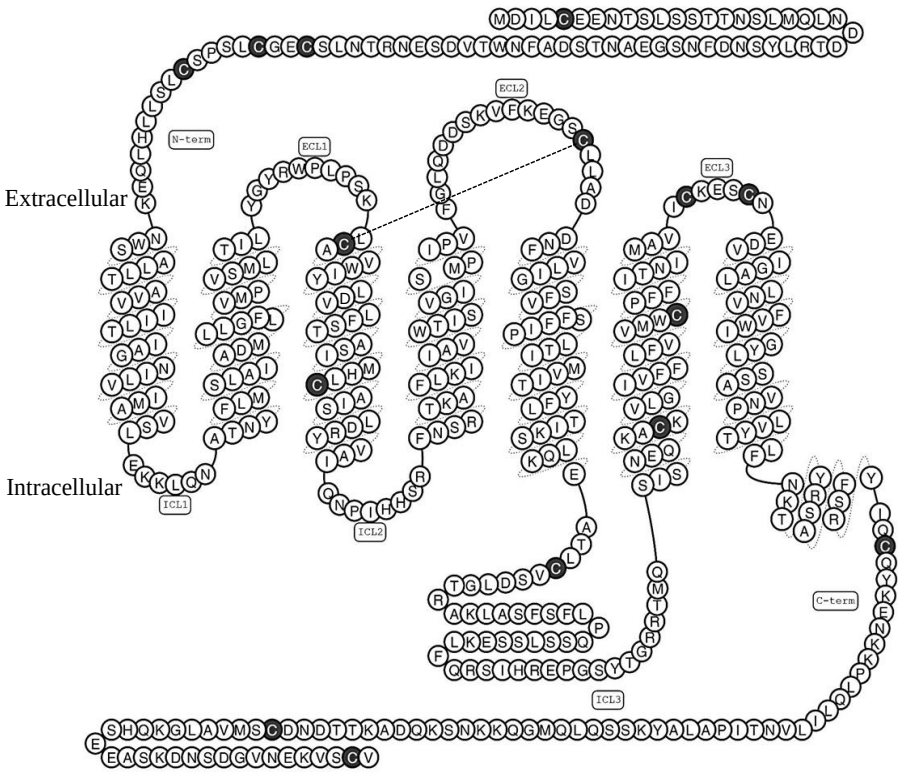
Extracellular
Intracellular
N-term
ECL1
ECL2
ECL3
ICL1
ICL2
ICL3
C-term

Figure 2

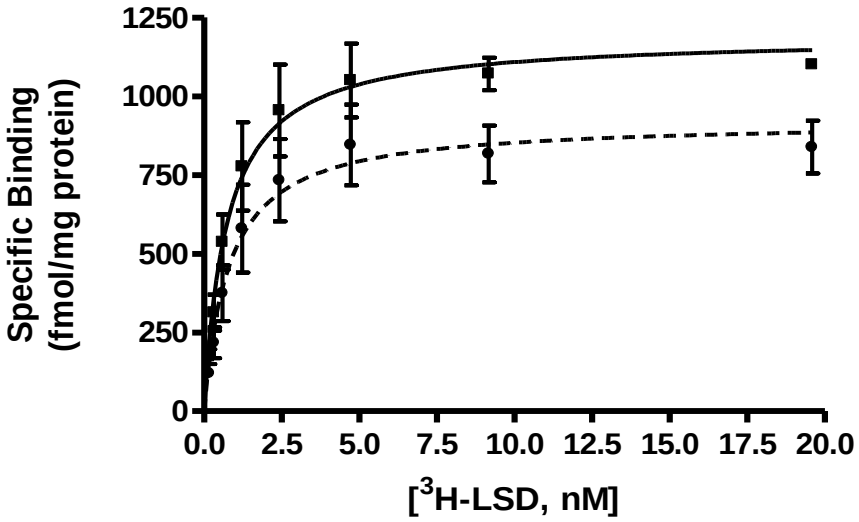
Specific Binding
(fmol/mg protein)
1250
1000
750
500
250
0
0.0
2.5
5.0
7.5
10.0
12.5
15.0
17.5
20.0
[3H-LSD, nM]

Figure 3

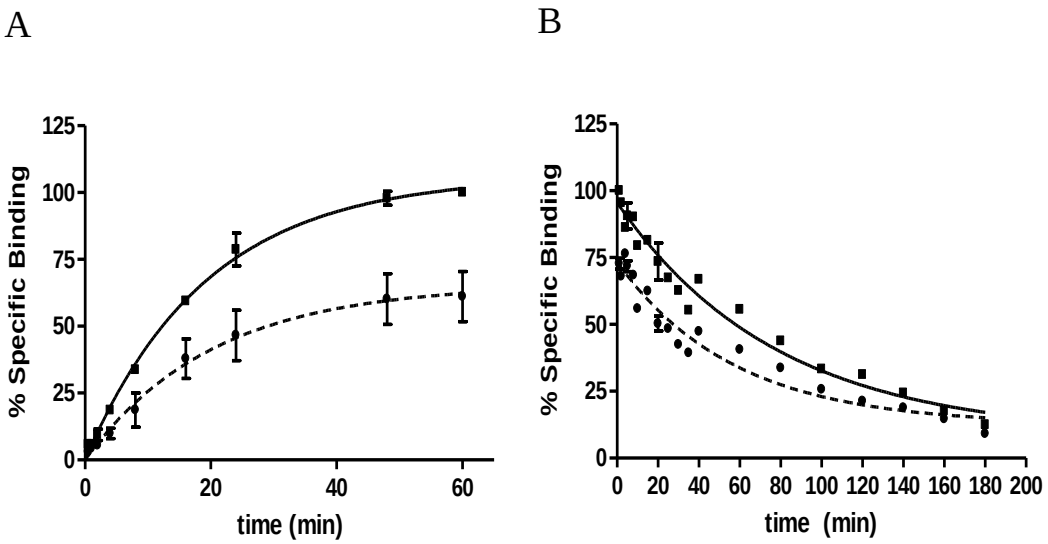
A
B
% Specific Binding
125
100
75
50
25
0
0
20
40
60
time (min)
% Specific Binding
125
100
75
50
25
0
0
20
40
60
80
100
120
140
160
180
200
time (min)

Figure 4

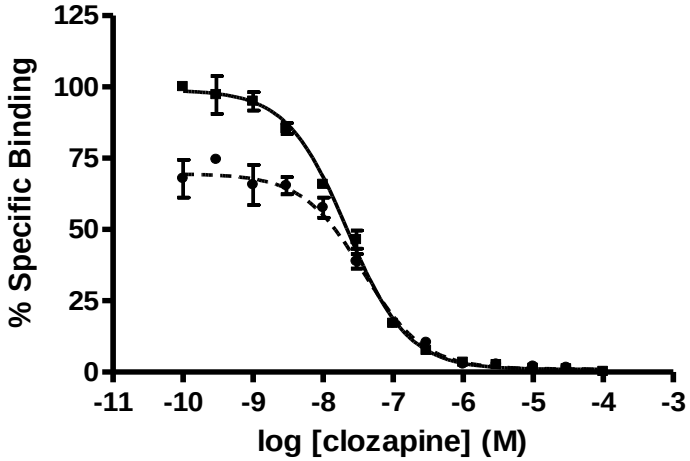
125
100
75
50
25
0
% Specific Binding
-11
-10
-9
-8
-7
-6
-5
-4
-3
log [clozapine] (M)

Figure 5

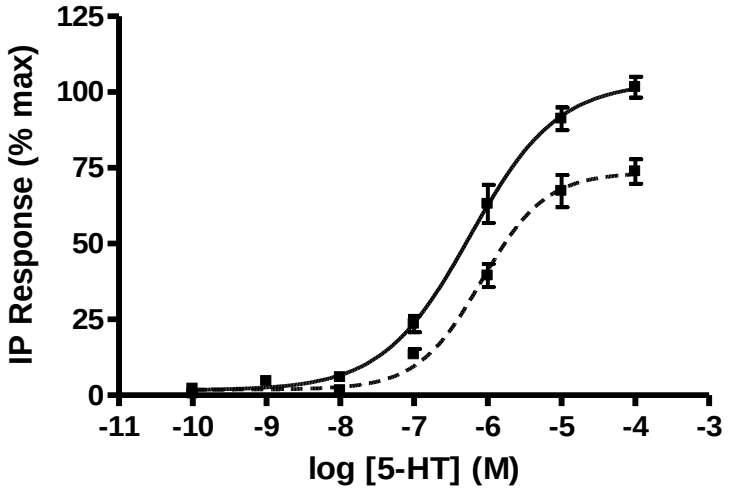

Figure 6

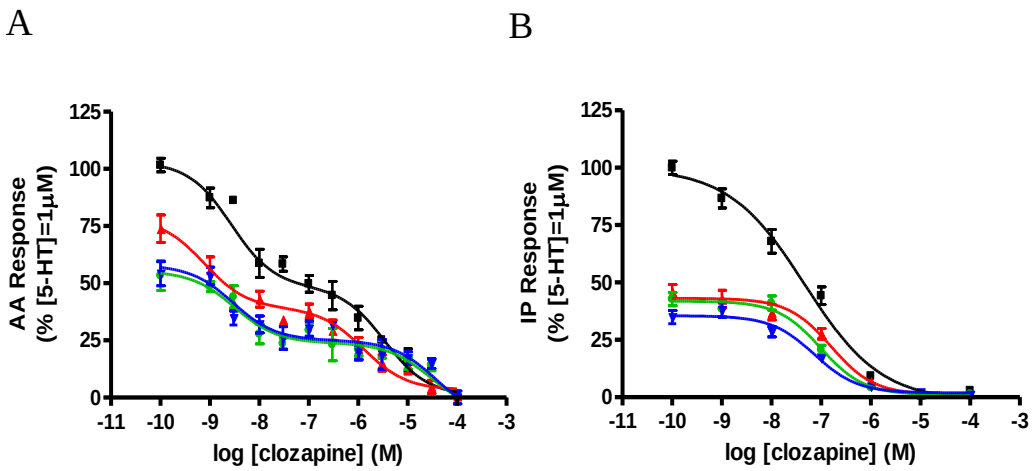
A
B
AA Response
(% [5-HT]=1μM)
IP Response
(% [5-HT]=1μM)
125
100
75
50
25
0
-11
-10
-9
-8
-7
-6
-5
-4
-3
log [clozapine] (M)

Figure 7

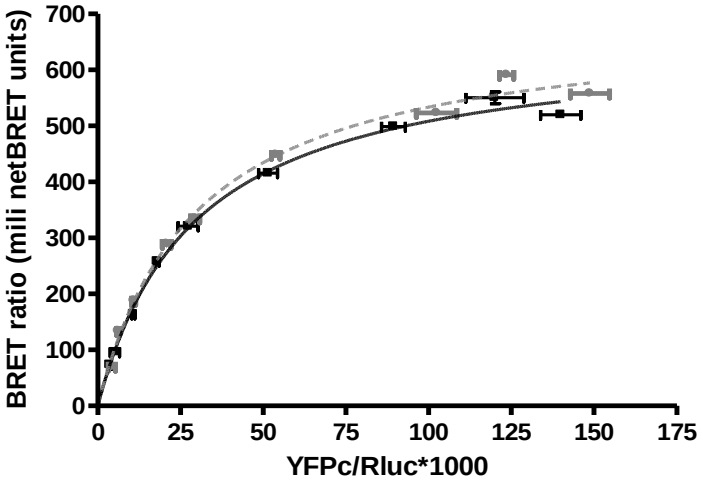
BRET ratio (mili netBRET units)
700
600
500
400
300
200
100
0
0
25
50
75
100
125
150
175
YFPc/Rluc*1000

Figure 8